

# Associated Production of Single Top Quark and W-boson Through Anomalous Couplings at LHeC based $\gamma p$ Colliders

I. T. Cakir\*

*Ankara University, Department of Physics, 06100, Ankara, Turkey*

A. Senol†

*Kastamonu University, Department of Physics,  
37100, Kuzeykent, Kastamonu, Turkey and*

*Abant Izzet Baysal University, Department of Physics, 14280, Bolu, Turkey*

A. T. Tasçi‡

*Kastamonu University, Department of Physics,  
37100, Kuzeykent, Kastamonu, Turkey*

## Abstract

We consider the production of a single top quark in association with a  $W$  boson at LHeC based  $\gamma p$  collider. We compute the cross section for the process  $\gamma p \rightarrow WtX$  with the anomalous  $Wtb$  and  $Wtb\gamma$  couplings. We find that the sensitivities to anomalous couplings of top quark are shown to be comparable, even better than the ones obtained from direct searches at hadron colliders.

---

\*Electronic address: [ilkay.turkcakir@gmail.com](mailto:ilkay.turkcakir@gmail.com)

†Electronic address: [asenol@kastamonu.edu.tr](mailto:asenol@kastamonu.edu.tr)

‡Electronic address: [atasci@kastamonu.edu.tr](mailto:atasci@kastamonu.edu.tr)

## I. INTRODUCTION

The considerable successes of top quark physics have entered into the field of precision measurements with the operation of Large Hadron Collider (LHC). Due to the large mass, close to the scale of electroweak symmetry breaking, the top quark is expected to be the most sensitive to new physics beyond the Standard Model (SM). In the SM, the top quark ( $t$ )-bottom quark ( $b$ )- $W$  boson interaction vertex is defined by the strength  $gF_{1L}/\sqrt{2}$  in which the coupling  $F_{1L}$  reduces to the quark mixing element  $V_{tb} \simeq 1$  at tree level. Corrections to this coupling, as well as non-zero anomalous couplings  $F_{1R}$ ,  $F_{2L}$  and  $F_{2R}$  can be generated by the new physics.

The direct constraints on the anomalous  $Wtb$  couplings, using the cross section measurement provided by CMS [1] and ATLAS [2] for t- channel single top quark production and measurement of decay asymmetries of top quark by ATLAS [3], are given in the region (-0.55, 0.65) for  $F_{1R}$ , (0.55, 1.55) for  $F_{1L}$ , (-0.70, 0.25) for  $F_{2R}$  and (-0.60, 0.55) for  $F_{2L}$  [4]. The Tevatron put more stringent bounds on these couplings as  $|F_{1R}|^2 < 0.30$ ,  $|F_{2L}|^2 < 0.05$  and  $|F_{2R}|^2 < 0.12$  assuming  $F_{1L} = 1$  at 95 % C.L. [5]. On the other hand, the indirect constraint from  $b \rightarrow s\gamma$  data by CLEO is  $|F_{1R}| < 4 \times 10^{-3}$  at  $2\sigma$  level [6]. From  $B^0 - \bar{B}^0$  mixings and rare  $B$  decay observables, it is apparent that indirect constraints are more restrictive than direct constraints for some of the anomalous couplings [7].

Extensive studies on the anomalous  $Wtb$  couplings described by a model independent effective Lagrangian approach have been performed in the literature through single and pair production of top quarks at hadron colliders [8–22] at lepton colliders [23–34] and at  $ep$  colliders [34].

A high energy electron-proton collider [35] can be realised by accelerating electrons in a linear accelerator (linac) to 60-140 GeV and colliding them with the 7 TeV protons circulating at the LHC. When the electron beam is accelerated by a linac, it can be converted into a beam of high energy real photons, by backscattering off laser photons. The spectrum of high energy photons would be about 80% of the energy of the initial electrons. It has the advantage of obtaining a 80-90% polarized electron beam and an intensive high energy photons. An operation of the LHeC as a  $\gamma p$  collider offers interesting possibilities to study TeV scale physics complementary to its  $ep$  option and to the LHC. The production of top quark by FCNC interactions at the LHeC based  $\gamma p$  collider has been studied in [36].

In this work, we investigate the associated production of single top quark and  $W$  boson through anomalous couplings at the LHeC based  $\gamma p$  collider. It is important to test the couplings of the top quark with the precision measurement at different energy scale, which can point the new physics beyond the SM. Therefore, the aim of this study is to provide bounds on the anomalous couplings of  $Wtb$  and  $Wtb\gamma$  vertices including corrections from dimension-six gauge invariant operators at the TeV scale.

## II. ANOMALOUS INTERACTIONS

The  $Wtb$  coupling is vector-axial (V-A) type in the SM. Therefore, only the left-handed fermion fields couple to the  $W$  boson. The result of this allows only a left-handed top quark to decay into a bottom quark and a  $W$  boson. However, the new physics can generate other possible  $Wtb$  couplings. The anomalous  $Wtb$  couplings can be expressed in a model independent effective Lagrangian approach [37]. Furthermore, upon electroweak symmetry breaking there is another quartic interaction vertex  $Wtb\gamma$  giving rise to the anomalous interactions. We consider the following model independent effective Lagrangian in the unitary gauge including anomalous  $Wtb$  and  $Wtb\gamma$  vertices with four independent form factor:

$$L = -\frac{g_W}{\sqrt{2}} \bar{b} \left[ \gamma^\mu (F_{1L} P_L + F_{1R} P_R) W_\mu^- + \frac{i\sigma^{\mu\nu}}{2m_W} (F_{2L} P_L + F_{2R} P_R) (q_\nu W_\mu^- - q_\mu W_\nu^- + g_e (A_\mu W_\nu^- - A_\nu W_\mu^-)) \right] t + h.c. \quad (1)$$

where left-handed (right-handed) projection operator is  $P_{L/R} = \frac{1}{2}(1 \mp \gamma_5)$ , and  $\sigma^{\mu\nu} = \frac{i}{2}(\gamma^\mu\gamma^\nu - \gamma^\nu\gamma^\mu)$ .  $q_\nu$  is the four-momentum of  $W$  boson,  $A_\mu(W_\mu)$  denotes photon field ( $W$  boson field),  $F_{iL/R}$  are complex dimensionless form factors. In the SM, the couplings  $F_{1R} = F_{2L} = F_{2R} = 0$  and  $F_{1L}$  is equal to CKM matrix element  $V_{tb}$ , which close to unity. The same argument can be applied for  $F_{1L} = V_{tq}$  where  $q = d, s$  when  $b$  quark is replaced by  $d$  or  $s$  quarks in the Lagrangian. In our calculation, we assume the  $F_{iL/R}$ 's to be real for simplicity and define  $F_{1L} = \Delta F_{1L} + 1$ .

For numerical calculations, the anomalous interaction vertices given in the effective Lagrangian are implemented into the CalcHEP [38] package. We use the spectrum of photons scattered backward from the interaction of laser light with the high energy electron beam [39] and the parton distribution function from CTEQ6M [40] within this package.

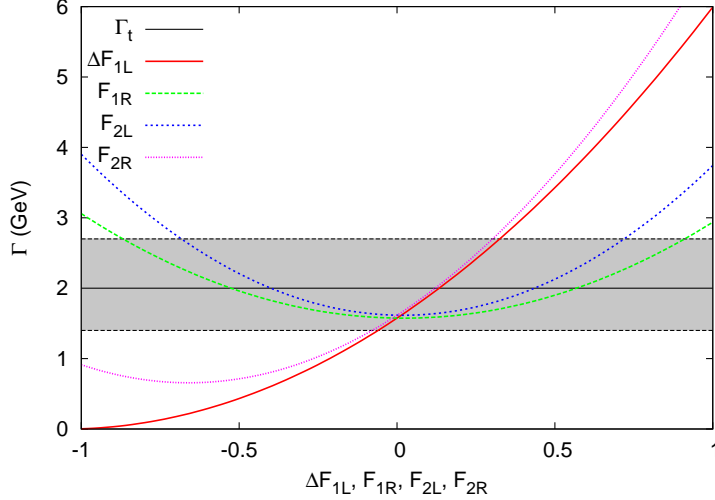


Figure 1: Decay width of the top quark depending on the anomalous couplings  $F_{1L}$ ,  $F_{1R}$ ,  $F_{2L}$  and  $F_{2R}$ .

Since top quark decay dominantly via the mode  $t \rightarrow Wb$  which deserves special attention, we first take into account top quark decay width  $\Gamma(t \rightarrow Wb)$  in the presence of anomalous couplings and find the decay width as:

$$\Gamma(t \rightarrow Wb) = \frac{g_e^2(m_t^2 - m_W^2)^2}{64\pi \sin^2 \theta_W m_t^3 m_W^2} [(F_{1L}^2 + 2F_{2L}^2 + F_{1R}^2 + 2F_{2R}^2)m_t^2 + (2F_{1L}^2 + F_{2L}^2 + 2F_{1R}^2 + F_{2R}^2)m_W^2 + 6(F_{1R}F_{2L} + F_{1L}F_{2R})m_t m_W] \quad (2)$$

Fig. 1 shows the decay width of top quark depending on the anomalous couplings by varying one of these couplings at a time while putting the others equal to zero. The solid line (black) in this figure denotes the average value of the experimental total decay width of top quark  $\Gamma_t = 2.0^{+0.7}_{-0.6}$  [41]. The dashed horizontal lines (black) shows the statistical errors within  $1\sigma$  around the average value. It is seen from Fig. 1 that the limits on the couplings:  $|F_{1R}| < 0.5$  and  $|F_{2L}| < 0.4$  can be extracted from the intersection point of the experimental average value of top quark decay width and the theoretical value calculated with the anomalous couplings. For the couplings  $\Delta F_{1L}$  and  $F_{2R}$ , assuming positive range, the limits can be found as  $\Delta F_{1L} < 0.2$  and  $F_{2R} < 0.2$ .

The related Feynman diagrams for the subprocess  $\gamma q \rightarrow W^- t$  are shown in Fig. 2, where  $q = d, s, b$ . The last diagram only contributes to the cross section when initial quark is a  $b$ -quark. The differential cross section for the subprocess is given by the formula

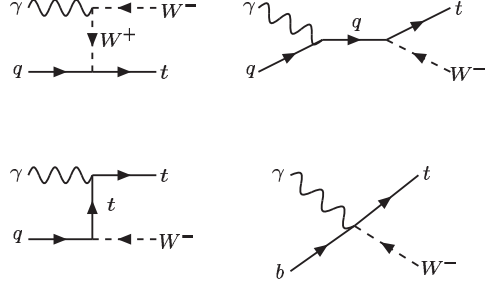


Figure 2: Representative Feynman diagrams for the subprocesses  $\gamma q \rightarrow W^- t$ , ( $q = d, s, b$ ).

$$\frac{d\hat{\sigma}}{d\hat{t}} = \frac{1}{16\pi\hat{s}^2} \sum_{i,j=1,2,3,4} < A_i A_j^* > \quad (3)$$

where  $< A_i A_j^* >$  is the average over initial state and sum over final state of the product of amplitudes  $A_i$  and  $A_j$  corresponding to the Feynman diagrams given in Fig. 2, and the Mandelstam variables are given as  $\hat{s} = (p_q + p_\gamma)^2$  and  $\hat{t} = (p_q - p_t)^2$  in terms of the four-momenta of particles. The explicit expressions for  $A_i A_j^*$  are given in the Appendix. The total cross section can be obtained by integrating differential cross section over the parton distribution functions and photon spectrum.

The total cross section for  $\gamma p \rightarrow W^- t X$  process depending on the energy of incoming electron beam is shown in Fig. 3. The cross sections for the coupling parameters  $F_{1R} = 0.5$ ,  $F_{2L} = 0.2$ ,  $F_{2R} = 0.2$  are larger than the cross section for the SM. In plotting Figs. 3, 4 and 5, one anomalous parameter is kept nonzero while the others are zero.

In Figs. 4 and 5, we present total cross section of  $\gamma p \rightarrow W^- t X$  as a function of anomalous couplings  $\Delta F_{1L}$ ,  $F_{1R}$ ,  $F_{2L}$  and  $F_{2R}$  with taking the energy of incoming electron to be  $E_e = 60$  GeV and  $E_e = 140$  GeV, respectively.

We calculate the cross section corresponding to the SM case for the anomalous couplings  $\Delta F_{1L} = 0$ ,  $F_{1R} = 0$ ,  $F_{2L} = 0$  and  $F_{2R} = 0$ . From Figs. 4 and 5, it is seen that the cross sections have minimum when  $F_{1R} = 0$ ,  $F_{2L} = 0$  and  $F_{2R} = 0$ , corresponding the values 0.47 pb and 1.809 pb for the center of mass energy  $\sqrt{s_{ep}} = 1.29$  TeV and  $\sqrt{s_{ep}} = 1.98$  TeV, respectively. With these figures, we observe the cross section, which shows symmetric behaviour around zero for the couplings  $F_{1R}$ ,  $F_{2L}$  and  $F_{2R}$  has approximately the same dependence to  $F_{2L}$  and  $F_{2R}$  couplings, and also the cross section enhances with increasing  $\Delta F_{1L}$ . The difference between the cross sections, when we set  $F_{2L} = 0.5$  or  $F_{2R} = 0.5$  and the SM value is about 75% as shown in Fig. 4, while it is 100% as in Fig. 5. However, the

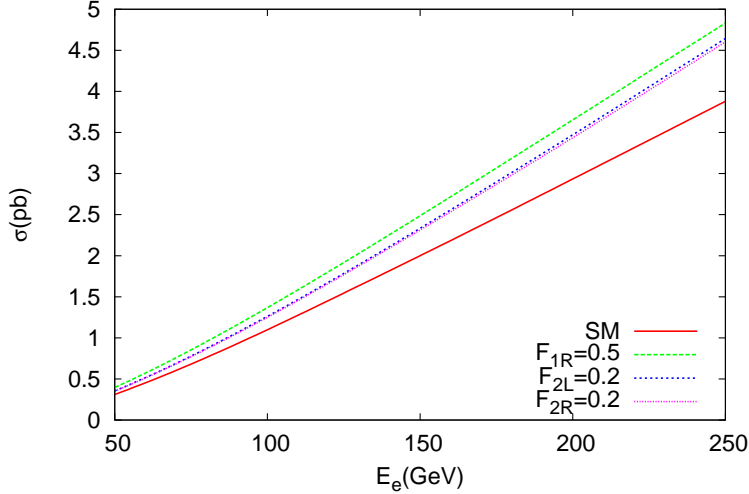


Figure 3: For the process  $\gamma p \rightarrow W^- t X$ , the dependence of cross section on the incoming electron beam energy.

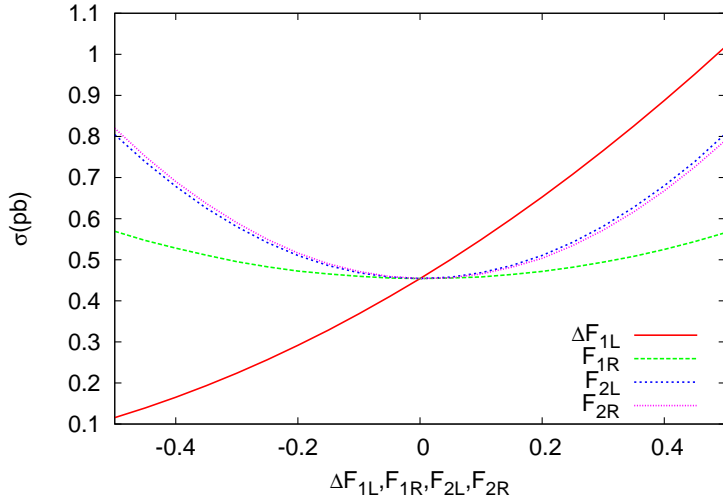


Figure 4: For the process  $\gamma p \rightarrow W^- t X$ , the dependence of cross section on anomalous couplings  $\Delta F_{1L}$ ,  $F_{1R}$ ,  $F_{2L}$  and  $F_{2R}$  for electron beam energy of 60 GeV.

cross sections changes slightly with  $F_{1R}$ .

### III. SENSITIVITY TO ANOMALOUS COUPLINGS

In this section, the sensitivity to the anomalous  $Wtb$  couplings is discussed taking into account the subprocesses  $\gamma q \rightarrow W^- t$  and  $\gamma \bar{q} \rightarrow W^+ \bar{t}$ , where  $q = d, s, b$ . We estimate

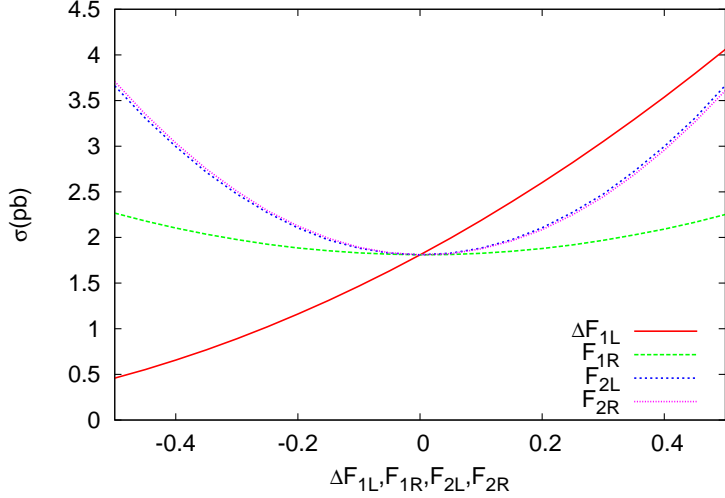


Figure 5: The same as the Fig. 4 but for electron beam energy of 140 GeV.

the sensitivity to these anomalous couplings at LHeC based  $\gamma p$  colliders for the integrated luminosities of 1, 10 and  $100 \text{ fb}^{-1}$ . We use  $\chi^2$  function to obtain sensitivity:

$$\chi^2 = \left( \frac{\sigma_{SM} - \sigma(\Delta F_{1L}, F_{1R}, F_{2L}, F_{2R})}{\Delta \sigma_{SM}} \right)^2 \quad (4)$$

where  $\Delta \sigma_{SM} = \sigma_{SM} \sqrt{\delta_{stat.}^2}$  with  $\delta_{stat.} = 1/\sqrt{N_{SM}}$ ,  $N_{SM}$  is the number of events calculated by  $N_{SM} = \sigma_{SM} \times BR(t \rightarrow W^+ b) \times BR(W^+ \rightarrow \text{hadrons}) \times BR(W^- \rightarrow l^- \nu) \times \epsilon_{b-tag} \times L_{int}$ . We take into account  $W^+$  boson decays hadronically while  $W^-$  decays leptonically corresponding to relevant branchings and assume b-jet tagging efficiency as 50%. In our calculations, we consider only one of the couplings is assumed to deviate from its SM value at a time.

The limits for the anomalous coupling parameters of top quark are given in Table I for integrated luminosities  $L_{int} = 1, 10, 100 \text{ fb}^{-1}$  and electron beam energy of 60 GeV. Table II presents the limits on these couplings for electron beam energy of 140 GeV. In these tables, the limits for the integrated luminosities of  $10 \text{ fb}^{-1}$  and  $100 \text{ fb}^{-1}$  are much better than the LHC results at  $\sqrt{s} = 7 \text{ TeV}$  [1, 3] and Tevatron results [5]. The expected precision limits of the anomalous top quark coupling measurements has been estimated as  $|\Delta F_{1L}| \lesssim 0.1$ ,  $|F_{1R}| \lesssim 0.3$ ,  $|F_{2L}| \lesssim 0.15$  and  $|F_{2R}| \lesssim 0.024$  [42] at the LHC with  $\sqrt{s} = 14 \text{ TeV}$  and  $L_{int} = 10 \text{ fb}^{-1}$ . The limits on the anomalous couplings found in this study can also be compared with the limits obtained from photon induced process in hadron-hadron collisions at the LHC [43]. The studies on anomalous  $Wtb$  couplings have shown the sensitivity for the

Table I: Sensitivity (95% C.L.) to anomalous  $Wtb$  couplings at the LHeC based  $\gamma p$  collider with electron beam energy of 60 GeV for various integrated luminosities.

$L(fb^{-1})$	$\Delta F_{1L}$	$F_{1R}$	$F_{2L}$	$F_{2R}$
1	-0.1088: +0.1318	-0.5258: +0.5328	-0.3010: +0.2995	-0.2903: +0.3106
10	-0.0187: +0.055	-0.3350: +0.3422	-0.1923: +0.1901	-0.1802: +0.2035
100	-0.0065: +0.0314	-0.1082: +0.1188	-0.0601: +0.0626	-0.1233: +0.1579

Table II: The same as the Table I, but for electron beam energy of 140 GeV.

$L(fb^{-1})$	$\Delta F_{1L}$	$F_{1R}$	$F_{2L}$	$F_{2R}$
1	-0.0617: +0.0581	-0.3416: +0.3490	-0.1705: +0.1684	-0.1643: +0.1781
10	-0.0187: +0.0172	-0.1884: +0.1957	-0.1014: +0.0939	-0.0871 : +0.1058
100	-0.0022: +0.0074	-0.1020: + 0.1118	-0.0524: +0.0554	-0.0453 : +0.0652

limits of  $-0.02 \lesssim F_{2L} \lesssim 0.06$  and  $|F_{2R}| \lesssim 0.05$  at linear collider with  $\sqrt{s} = 500$  GeV and  $L_{int} = 500 fb^{-1}$  [44, 45]. In this study, we find much better limits on the anomalous couplings of top quark as  $-0.0187 < \Delta F_{1L} < 0.0172$ ,  $-0.1884 < F_{1R} < 0.1957$ ,  $-0.1014 < F_{2L} < 0.0939$  and  $-0.0871 < F_{2R} < 0.1058$  at an integrated luminosity of  $10 fb^{-1}$  for the electron beam energy of 140 GeV at the LHeC based  $\gamma p$  collider.

#### IV. CONCLUSIONS

The precision measurement of the anomalous couplings relevant to  $Wtb$  and  $Wtb\gamma$  vertices is very important for the future experiments, and it can point the new physics beyond the SM. The limits on the couplings  $\Delta F_{1L}$  and  $F_{1R}$  are better than the limits from direct searches at Tevatron and LHC. However, the limits  $F_{2L}$  and  $F_{2R}$  become comparable to the results from LHC and high energy linear colliders. The measurement of single top production at LHeC based  $\gamma p$  collider would provide complementary information to the LHC data that could help in determining anomalous  $Wtb$  couplings. In addition to QCD explorer searches, the LHeC will contribute to top quark physics at high momentum transfer in deep inelastic scattering.

## Acknowledgments

Authors would like to thank O. Cakir for valuable suggestions and comments.

## Appendix

The explicit expressions for  $\langle A_i A_j^* \rangle$  corresponding to Feynman diagrams in Fig. 2 are following:

$$\begin{aligned} \langle |A_1|^2 \rangle = & -\frac{1}{16m_W^5 \sin\theta_W^2 (m_W^2 - t)^2} g_e^4 ((F_{2L} F_{1R} + F_{1L} F_{2R}) m_t (m_W^6 (20s - 13t) - t^3 (2s + t) \\ & - m_W^2 t^2 (4s + 13t) - m_W^4 t (22s + 47t) + m_t^2 (13m_W^6 + 47m_W^4 t - 13m_W^2 t^2 + t^3)) \\ & + (F_{2L}^2 + F_{2R}^2) m_W (4m_t^4 (m_W^4 + 4m_W^2 t - t^2) + t (5(m_W^3 - 2m_W s)^2 \\ & + (-13m_W^4 + 24m_W^2 s - 4s^2) t - (m_W^2 + 4s) t^2 + t^3) \\ & + m_t^2 (-5m_W^6 + t^2 (4s + 3t) - 3m_W^2 t (8s + 5t) + m_W^4 (20s + 9t))) \\ & + 2(F_{1L}^2 + F_{1R}^2) m_W (m_t^4 (7m_W^4 - 4m_W^2 t + t^2) + m_t^2 (2m_W^6 + 2m_W^2 t^2 + m_W^4 (s + t) \\ & - t^2 (s + t)) + 2m_W^2 (m_W^4 (5s - t) + t(s^2 + st + t^2) - m_W^2 (5s^2 + 6st + 4t^2)))) \end{aligned}$$

$$\begin{aligned} 2Re \langle A_1 A_2^* \rangle = & (g_e^4 (m_W^2 (F_{2R}^2 m_t^2 (8m_t^4 - 5m_W^4 + 2m_t^2 (7m_W^2 - 6s) + 5m_W^2 s + 4s^2) \\ & + F_{1R}^2 (4m_t^6 + m_t^4 (19m_W^2 - 7s) - m_t^2 s (7m_W^2 + s) + 2s (5m_W^4 - 6m_W^2 s + s^2))) \\ & - (F_{2R}^2 m_W^2 (10m_t^4 - 5m_W^4 + 3m_t^2 s + 11m_W^2 s - 4s^2) \\ & + F_{1R}^2 (m_t^4 (12m_W^2 - s) + 4m_W^2 (5m_W^2 - s) s + m_t^2 (7m_W^4 - 7m_W^2 s + s^2))) t \\ & + (F_{2R}^2 m_W^2 (-3m_t^2 - 14m_W^2 + 9s) + F_{1R}^2 (m_t^4 + m_t^2 (4m_W^2 - 2s) + 6m_W^2 (-2m_W^2 + s))) t^2 \\ & + (5F_{2R}^2 m_W^2 - F_{1R}^2 (m_t^2 - 4m_W^2)) t^3 + (F_{2L} F_{1R} + F_{1L} F_{2R}) m_t m_W (m_W^4 (3s - 20t) \\ & + 2m_t^4 (11m_W^2 + t) - 3(s - 2t) t (s + t) + m_W^2 (s^2 - 6st - 10t^2) \\ & + 4m_t^2 (5m_W^4 - 2t^2 - 3m_W^2 (2s + t))) + F_{2L}^2 m_W^2 (8m_t^6 + 2m_t^4 (7m_W^2 - 6s - 5t) \\ & + m_t^2 (-5m_W^4 + 5m_W^2 s + 4s^2 - 3st - 3t^2) + t (5m_W^4 + (s + t)(4s + 5t) - m_W^2 (11s + 14t))) \\ & + F_{1L}^2 (4m_t^6 m_W^2 + m_t^4 (19m_W^4 + t(s + t) - m_W^2 (7s + 12t)) - \\ & - m_t^2 (7m_W^4 (s + t) + t(s + t)^2 + m_W^2 (s^2 - 7st - 4t^2)) + 2m_W^2 (5m_W^4 s \\ & + (s + t)(s^2 + st + 2t^2) - 2m_W^2 (3s^2 + 5st + 3t^2)))) / (12m_W^4 \sin^2 \theta_W (m_W^2 - t) (m_W^2 - s - \end{aligned}$$

$$\begin{aligned}
2Re < A_1 A_3^* > = & \frac{1}{24m_W^4 \sin\theta_W^2 s(m_W^2 - t)} g_e^4 (m_W^2 (F_{2R}^2 m_t^2 (-8m_t^4 + 6m_t^2(m_W^2 + 2s) + (2m_W^2 - s)(m_W^2 + 4s)) \\
& + F_{1R}^2 (-4m_t^6 + 2(m_W^2 - s)s(4m_W^2 + s) + m_t^4(-4m_W^2 + 7s) + m_t^2(8m_W^4 + 4m_W^2s + s^2))) \\
& + F_{2R}^2 m_W^2 (6m_t^4 - 2m_W^4 + 3m_W^2s + 4s^2 - m_t^2(4m_W^2 + 9s)) \\
& + F_{1R}^2 (m_t^4 + (4m_W^2 - s) - 2m_W^2(4m_W^2 + s^2) + m_t^2(4m_W^4 - 3m_W^2s + s)))t \\
& + F_{1R}^2 (m_t^2 - 4m_W^2)s - F_{2R}^2 m_W^2 (-2m_t^2 + 2m_W^2 + s))t^2 + (F_{2L}F_{1R} + F_{1L}F_{2R})m_t m_W \\
& (2m_W^4(8s - 11t) + s(3s - 2t)t - 2m_t^4(11m_W^2 + t) - m_W^2(s^2 + 14st + 2t^2) \\
& + 2m_t^2(11m_W^4 + t^2 + 12m_W^2(s + t))) + F_{2L}^2 m_W^2 (-8m_t^6 + 6m_t^4(m_W^2 + 2s + t) \\
& + m_t^2(2m_W^4 - 4s^2 + m_W^2(7s - 4t) - 9st + 2t^2) - t(2m_W^4 + s(-4s + t) + m_W^2(-3s + 2t))) \\
& + F_{1L}^2 (-4m_t^6 m_W^2 + m_t^2(8m_W^6 + m_W^2s(s - 3t) + 4m_W^4(s + t) + st(s + t)) \\
& + m_t^4(-4m_W^4 - st + m_W^2(7s + 4t)) + (2m_W^2(-3m_W^2s^2 + 4m_W^4(s - t) - s(s^2 + st + 2t^2)))
\end{aligned}$$

$$\begin{aligned}
2Re < A_1 A_4^* > = & \frac{1}{16m_W^5 \sin\theta_W^2 (m_W^2 - t)} g_e^4 ((F_{2L}F_{1R} + F_{2R}F_{1L})mt \\
& (-12m_W^2t(s + t) + t^2(2s + t) + m_W^4(2s + 35t) - m_t^2(35m_W^4 - 12m_W^2t + t^2)) \\
& + (F_{2L}^2 + F_{2R}^2)m_W(8m_t^4(-3m_W^2 + t) + t((m_W^2 - 2s)^2 + 4(2m_W^2 + s)t - t^2)) \\
& - m_t^2(m_W^4 - 4m_W^2(s + 4t) + t(12s + 7t)))
\end{aligned}$$

$$\begin{aligned}
|A_2|^2 = & - \frac{1}{(9m_W^2 \sin\theta_W^2 (-m_W^2 + s + t)^2)} g_e^4 (2(F_{1R}^2 + 2F_{2R}^2)m_t^6 + 6(F_{1R}^2 + F_{2R}^2)m_t^4 m_W^4 \\
& -(2F_{1R}^2 + F_{2R}^2)m_t^2 m_W^4 - 4(F_{1R}^2 + 2F_{2R}^2)m_t^4 s - (5F_{1R}^2 + 4F_{2R}^2)m_t^2 m_W^2 s \\
& + 2(F_{1R}^2 + 2F_{2R}^2)m_W^4 s + 2(F_{1R}^2 + 2F_{2R}^2)m_t^2 s^2 - (2F_{1R}^2 + F_{2R}^2)m_W^2 s^2 + \\
& + 6(F_{2L}F_{1R} + F_{1L}F_{2R})m_t m_W(m_t^2 - s - t)(2m_t^2 + m_W^2 - s - t) \\
& + (F_{2R}^2(-8m_t^4 + 2m_W^4 - 2m_t^2(m_W^2 - 3s) - 5m_W^2s + 2s^2) + F_{1R}^2 \\
& (-4m_t^4 + m_W^4 - 4m_W^2s + s^2 + m_t^2(-4m_W^2 + 3s)))t \\
& + (F_{1R}^2 + 2F_{2R}^2)(m_t^2 - 2m_W^2 + 2s + t)t^2 + F_{2L}^2(4m_t^6 + m_t^4(6m_W^2 - 8(s + t)) \\
& - 2m_t^2(m_W^4 + m_W^2(2s + t) - (s + t)(2s + t)) + (m_W^2 - s - t)(-2t(s + t) + m_W^2(s + 2t))) \\
& + F_{1L}^2(2m_t^6 + m_t^4(6m_W^2 - 4(s + t)) + (m_W^2 - s - t)(-t(s + t) + m_W^2(2s + t))) \\
& + m_t^2(-m_W^4 + (s + t)(2s + t) - m_W^2(5s + 4t)))
\end{aligned}$$

$$\begin{aligned}
2Re < A_2 A_3^* > = & - \frac{1}{9m_W^2 \sin\theta_W^2 s(-m_W^2 + s + t)} g_e^4 (F_{1R}^2 m_t^4 (m_t^2 + m_W^2) + F_{2R} M_t^4 (2m_t^2 - m_W^2) \\
& - 2F_{1R}^2 m_t^2 (m_W^4 + m_t^2 s) - F_{2R}^2 m_t^2 (m_W^4 + 4m_t^2 s) - (F_{1R}^2 + F_{2R}^2) m_t^2 m_W^2 s + F_{2R}^2 m_W^2 s (s - m_W^2) \\
& + (F_{1R}^2 + 2F_{2R}^2) m_t^2 s^2 + (-F_{2R}^2 (2m_t^2 + m_W^2) (m_t^2 - m_W^2 - s) - F_{1R}^2 (m_t^2 + m_t^4 m_W^2 \\
& - 2m_W^4 + m_W^2 s - s^2)) t + F_{1R}^2 s t^2 + (F_{2L} F_{1R} + F_{1L} F_{2R}) m_t m_W (6m_t^4 - m_W^2 (s - 6t) \\
& - 3m_t^2 (2m_W^2 + 3s + 2t) + s(3s + 4t)) + F_{1L}^2 (m_t^6 + m_t^4 (m_W^2 - 2s - t) \\
& - m_t^2 (2m_W^4 - s^2 + m_W^2 (s + t)) + t(2m_W^4 - m_W^2 s + s(s + t))) \\
& + F_{2L}^2 (2m_t^6 - m_t^2 (m_W^2 + 2s) (m_W^2 - s - t) - m_t^4 (m_W^2 + 4s + 2t) + m_W^2 (m_W^2 (-s + t) + s(s + t)))
\end{aligned}$$

$$\begin{aligned}
2Re < A_2 A_4^* > = & \frac{1}{6m_W^3 \sin\theta_W^2 (m_W^2 - s - t)} g_e^4 ((F_{2L}^2 + F_{2R}^2) m_W (5m_t^4 - 2(s + t)^2 + m_W^2 (2s + t) \\
& - m_t^2 (m_W^2 + 3(s + t))) + (F_{2L} F_{1R} + F_{2R} F_{1L}) m_t (m_t^4 + (s + t)(s + 3t) \\
& - m_W^2 (7s + 8t) + m_t^2 (8m_W^2 - 2(s + 2t)))) 
\end{aligned}$$

$$\begin{aligned}
|A_3|^2 = & \frac{1}{36m_W^2 \sin\theta_W^2 s} g_e^4 (m_W^2 (-(F_{1L}^2 + 2F_{2L}^2 + F_{1R}^2 + 2F_{2R}^2) m_t^2 - 6(F_{2L} F_{1R} + F_{1L} F_{2R}) m_t m_W \\
& + (2F_{1L}^2 + F_{2L}^2 + 2F_{1R}^2 + F_{2R}^2) (s - m_W^2)) + ((F_{1R}^2 + 2F_{2R}^2) m_t^2 + 6(F_{2L} F_{1R} + F_{1L} F_{2R}) m_t m_W \\
& + (2F_{1R}^2 + F_{2R}^2) m_W^2 + F_{2L}^2 (2m_t^2 + m_W^2 - 2s) + F_{1L}^2 (m_t^2 + 2m_W^2 - s) \\
& - (F_{1R}^2 + 2F_{2R}^2) s) t)
\end{aligned}$$

$$\begin{aligned}
2Re < A_3 A_4^* > = & - \frac{1}{12m_W^3 s^2 \sin\theta_W^2} g_e^4 ((F_{2L} F_{1R} + F_{2R} F_{1L}) m_t (m_t^4 + m_W^2 (-4s + t) + s(s + t) \\
& - m_t^2 (m_W^2 + 2s + t)) + (F_{2L}^2 + F_{2R}^2) m_W (m_t^4 + 2s^2 + m_W^2 (-2s + t) \\
& - m_t^2 (m_W^2 + 3s + t)))
\end{aligned}$$

$$|A_4|^2 = \frac{1}{8m_W^4 \sin\theta_W^2} g_e^4 (F_{2L}^2 + F_{2R}^2) (2m_t^4 + 2s(s + t) - m_W^2 (2s + t) + m_t^2 (m_W^2 - 2(2s + t)))$$


---

[1] CMS Collaboration, note CMS-PAS-TOP-10-008. G. Aad *et al.* [Atlas Collaboration], note ATLAS-CONF- 2011-027.

- [2] G. Aad *et al.* [Atlas Collaboration], note ATLAS-CONF- 2011-027.
- [3] G. Aad *et al.* [Atlas Collaboration], note ATLAS-CONF- 2011-037.
- [4] J. A. Aguilar-Saavedra, N. F. Castro and A. Onofre, Phys. Rev. D **83**, 117301 (2011) [arXiv:1105.0117 [hep-ph]].
- [5] V. M. Abazov *et al.* [D0 Collaboration], Phys. Lett. B **713**, 165 (2012) [arXiv:1204.2332 [hep-ex]].
- [6] F. Larios, M. A. Perez and C. P. Yuan, Phys. Lett. B **457**, 334 (1999) [hep-ph/9903394].
- [7] J. Drobna, S. Fajfer, and J. F. Kamenik, Nucl. Phys. B **855**, 82 (2012).
- [8] D. O. Carlson and C. P. Yuan, Phys. Lett. B **306**, 386 (1993).
- [9] D. O. Carlson, E. Malkawi and C. P. Yuan, Phys. Lett. B **337**, 145 (1994) [hep-ph/9405277].
- [10] T. Stelzer and S. Willenbrock, Phys. Lett. B **357**, 125 (1995) [hep-ph/9505433].
- [11] A. Heinson, A. S. Belyaev and E. E. Boos, Phys. Rev. D **56**, 3114 (1997) [hep-ph/9612424].
- [12] E. Boos, L. Dudko and T. Ohl, Eur. Phys. J. C **11**, 473 (1999) [hep-ph/9903215].
- [13] F. del Aguila and J. A. Aguilar-Saavedra, Phys. Rev. D **67**, 014009 (2003) [hep-ph/0208171].
- [14] M. M. Najafabadi, JHEP **0803**, 024 (2008) [arXiv:0801.1939 [hep-ph]].
- [15] J. A. Aguilar-Saavedra, Nucl. Phys. B **804**, 160 (2008) [arXiv:0803.3810 [hep-ph]].
- [16] S. K. Gupta, A. S. Mete and G. Valencia, Phys. Rev. D **80**, 034013 (2009) [arXiv:0905.1074 [hep-ph]].
- [17] E. L. Berger, Q. -H. Cao and I. Low, Phys. Rev. D **80**, 074020 (2009) [arXiv:0907.2191 [hep-ph]].
- [18] C. Zhang and S. Willenbrock, Phys. Rev. D **83**, 034006 (2011) [arXiv:1008.3869 [hep-ph]].
- [19] S. D. Rindani and P. Sharma, JHEP **1111**, 082 (2011) [arXiv:1107.2597 [hep-ph]].
- [20] S. D. Rindani and P. Sharma, Phys. Lett. B **712**, 413 (2012) [arXiv:1108.4165 [hep-ph]].
- [21] K. Kolodziej, Phys. Lett. B **710**, 671 (2012) [arXiv:1110.2103 [hep-ph]].
- [22] K. Kolodziej, arXiv:1212.6733 [hep-ph].
- [23] S. Ambrosanio and B. Mele, Z. Phys. C **63**, 63 (1994) [hep-ph/9311263].
- [24] N. V. Dokholian and G. V. Jikia, Phys. Lett. B **336**, 251 (1994).
- [25] K. Hagiwara, M. Tanaka and T. Stelzer, Phys. Lett. B **325**, 521 (1994) [hep-ph/9401295].
- [26] E. Boos, M. Sachwitz, H. J. Schreiber, S. Shichanin, A. Pukhov, V. Ilin, T. Ishikawa and T. Kaneko *et al.*, Phys. Lett. B **326**, 190 (1994).
- [27] E. Boos, M. Dubinin, M. Sachwitz and H. J. Schreiber, Eur. Phys. J. C **16**, 269 (2000)

[hep-ph/0001048].

- [28] B. Grzadkowski and Z. Hioki, Nucl. Phys. B **585**, 3 (2000) [hep-ph/0004223].
- [29] E. Boos, M. Dubinin, A. Pukhov, M. Sachwitz and H. J. Schreiber, Eur. Phys. J. C **21**, 81 (2001) [hep-ph/0104279].
- [30] K. Cieckiewicz and K. Kolodziej, Acta Phys. Polon. B **34**, 5497 (2003) [hep-ph/0310300].
- [31] K. Kolodziej, Phys. Lett. B **584**, 89 (2004) [hep-ph/0312168].
- [32] P. Batra and T. M. P. Tait, Phys. Rev. D **74**, 054021 (2006) [hep-ph/0606068].
- [33] B. Sahin and I. Sahin, Eur. Phys. J. C **54**, 435 (2008) [arXiv:0709.0365 [hep-ph]].
- [34] S. Atag, O. Cakir and B. Dilec, Phys. Lett. B **522**, 76 (2001) [hep-ph/0107179].
- [35] J. L. Abelleira Fernandez *et al.*, LHeC Study Group, J. Phy. G: Nucl. Part. Phys. **39**, 075001 (2012).
- [36] İ. T. Cakir, O. Cakir and S. Sultansoy, *et al.* Phys. Let. B **685**, 170 (2010).
- [37] J. A. Aguilar-Saavedra, Nucl. Phys. B **812**, 181 (2009); J. M. Yang, B. Young, Phys. Rev. D **56**, 5907 (1997).
- [38] A. Pukhov *et al.*, arXiv:hep-ph/9908288, (1999); A. Pukhov, arXiv:hep-ph/0412191, (2004).
- [39] I. F.Ginzburg, G.L.Kotkin, V.G.Serbo and V.I.Telnov, Nucl. Instrum. Meth. **205**, 47 (1983).
- [40] J. Pumplin *et al.*, JHEP **0207**, 012 (2002). arXiv:hep-ph/0201195.
- [41] J. Beringer *et al.* [Particle Data Group Collaboration], Phys. Rev. D **86**, 010001 (2012).
- [42] F.Bach, T. Ohl, Phys. Rev. D **86**, 114026 (2012).
- [43] B. Sahin, A. Billur, Phys.Rev. D **86** 074026 (2012).
- [44] E. Devetak, A. Nomerotski, Phys. Rev. D **84**, 034029 (2011).
- [45] E. Boos *et al.*, Eur. Phys. J. C **21**, 81–91 (2001).